METHODS AND APPROACHES

Illuminating cell signaling with genetically encoded FRET biosensors in adult mouse cardiomyocytes

Gopireddy Raghavender Reddy[1]*, Toni M. West[1]* (ID), Zhong Jian[1], Mark Jaradeh[1] (ID), Qian Shi[1], Ying Wang[1], Ye Chen-Izu[1,2,3] (ID), and Yang K. Xiang[1,4] (ID)

FRET-based biosensor experiments in adult cardiomyocytes are a powerful way of dissecting the spatiotemporal dynamics of the complicated signaling networks that regulate cardiac health and disease. However, although much information has been gleaned from FRET studies on cardiomyocytes from larger species, experiments on adult cardiomyocytes from mice have been difficult at best. Thus the large variety of genetic mouse models cannot be easily used for this type of study. Here we develop cell culture conditions for adult mouse cardiomyocytes that permit robust expression of adenoviral FRET biosensors and reproducible FRET experimentation. We find that addition of 6.25 μM blebbistatin or 20 μM (*S*)-nitro-blebbistatin to a minimal essential medium containing 10 mM HEPES and 0.2% BSA maintains morphology of cardiomyocytes from physiological, pathological, and transgenic mouse models for up to 50 h after adenoviral infection. This provides a 10–15-h time window to perform reproducible FRET readings using a variety of CFP/YFP sensors between 30 and 50 h postinfection. The culture is applicable to cardiomyocytes isolated from transgenic mouse models as well as models with cardiac diseases. Therefore, this study helps scientists to disentangle complicated signaling networks important in health and disease of cardiomyocytes.

Introduction

FRET-based biosensors are powerful tools for studying intracellular signaling on a single cell, showing time-dependent nuances in cellular changes. But the live-cell imaging–based FRET assays have some limitations in adult cardiomyocytes. Namely, it normally takes ∼35 h of adenoviral infection to produce enough expression of the biosensor protein to allow effective performance of the FRET assay. This has been a critical limitation in studying adult cardiomyocytes. Up until now, culture of isolated adult cardiomyocytes from larger animals such as pigs, rabbits, and rats has been effective for FRET assays (Nikolaev et al., 2010; Barbagallo et al., 2016; Fields et al., 2016; Wang et al., 2017). But it has been difficult to culture isolated adult cardiomyocytes from mice because they either enter apoptosis or dedifferentiate over a 35–50-h period needed for FRET sensor expression. In other species' cardiomyocytes, it has been found that calcium tolerance and cell attachment to the substrate are two important factors for generating long-term cultures (Louch et al., 2011), and it is thought that calcium intolerance plays an important role in mouse cardiomyocyte toxicity in long-term cultures (Bers, 2002). Hence, the limitations of mouse cardiomyocyte extended culture morphology has made adult mouse cardiomyocyte FRET difficult at best.

To overcome this major challenge, the Nikolaev laboratory has developed transgenically expressed FRET sensors in mice (Götz et al., 2014; Sprenger et al., 2015). This is an important contribution to overcoming a large hurdle, but these sensors have low signal-to-noise ratio because of poor expression. Additionally, a new mouse genetic line must be developed for each sensor, which is expensive and time intensive. Furthermore, exploring the ramification of any genetic knockout mouse model with FRET methods means additionally crossbreeding the mice together, which lengthens the time for the experiment greatly and may be financially prohibitive. Because of these limitations, many avenues of research remain untouched because the myriad of available transgenic mouse models are inaccessible.

Previous attempts have also been made to culture adult mouse cardiomyocytes for FRET. We have previously reported a method for performing FRET with the PKA biosensor AKAR2.2 on WT adult mouse cardiomyocytes where cells were cultured in MEM containing 2.5% FBS for 24 h after infection (Soto et al., 2009). The Nikolaev group has reported a similar method for performing FRET measurements of cAMP ∼24 h after biosensor transfection on WT adult mouse cardiomyocytes where the cells are cultured in MEM containing 0.1 mg/ml BSA (Börner et al., 2011) but has since moved to using the transgenically modified FRET sensor–expressing mice. The Zaccolo group also reported a technique for performing FRET on adult mouse cardiomyocytes

[1]Department of Pharmacology, University of California at Davis, Davis, CA; [2]Department of Bioengineering, University of California at Davis, Davis, CA; [3]Department of Internal Medicine/Cardiology, University of California at Davis, Davis, CA; [4]Veterans Affairs Northern California Health Care System, Mather, CA.

*G.R. Reddy and T.M. West contributed equally to the production of this paper; Correspondence to Yang K. Xiang: ykxiang@ucdavis.edu.

where cytochalasin D is implemented to improve cell morphology at 24 h after infection (Lomas et al., 2015). For these studies, because the FRET assay is done 24 h after infection, the signal-to-noise ratio is poor; and still, there are difficulties getting a large number of data points because of low numbers of surviving cells (Lomas et al., 2015). We hypothesized that using a tried-and-true method for FRET biosensor expression—that of adenovirus infection—combined with an optimized culturing condition would be able to solve these problems effectively. In the present study, we have found a method for culturing and infecting isolated adult cardiomyocytes from mice to effectively do FRET analysis.

In initial trials, A kinase activity reporter 3 (AKAR3; Allen and Zhang, 2006) was implemented as the biosensor to show proof of principle and to optimize the culture conditions. AKAR3 is a cyan fluorescent protein/yellow fluorescent protein (CFP/YFP) sensor that detects PKA activity (Allen and Zhang, 2006; Ni et al., 2006). Once conditions for FRET using AKAR3 were established in adult mouse cardiomyocytes, other CFP/YFP sensors of Epac-S^{H187} (Klarenbeek et al., 2015), cGMP indicator-500 nM (cGi500; Russwurm et al., 2007), and Camui (Takao et al., 2005) were also effectively used. These sensors detect cAMP concentration, cGMP concentration, and calcium/calmodulin-dependent kinase II (CaMKII) activity, respectively. In our culture, overall morphology, sarcomere length, and a majority of protein expression profiles tested did not significantly change over the culturing period, signifying that signaling networks are well maintained under this protocol. Moreover, AKAR3 was expressed in cardiomyocytes from transgenic *β-1 adrenergic receptor* knockout mice (β1KO), and differential responses to isoproterenol could be observed. Finally, AKAR3 was expressed in cardiomyocytes from healthy and diabetic animals, and differential responses to isoproterenol could be observed in diabetic cardiomyocytes compared with normal cells. Fig. 1 A depicts a flow chart of the method to perform FRET on adult mouse cardiomyocytes. The future utilization of FRET biosensors in a variety of transgenic mouse cardiomyocytes will permit researchers to broadly explore cardiomyocyte signaling cascades important in health and disease in hearts.

Materials and methods

Animal welfare
All animal care and experimentation followed National Institutes of Health (NIH) guidelines and were approved by the University of California Davis Institutional Animal Care and Use Committee. Animals were euthanized under general anesthesia (induction with 2–5% isoflurane in 100% oxygen until reflex to toe pinch was not present).

Reagents and materials
All reagents and materials were obtained from Millipore-Sigma unless otherwise specified.

Cardiomyocyte isolation methods
Three different techniques for isolating adult mouse cardiomyocytes were assessed for FRET culture, where cardiomyocytes were separated from other cell types. In all cases, only cardiomyocytes could be observed in the cultures; no other cell types were detected. For a majority of the mouse experimentation, cardiomyocytes from 8–10-wk-old male WT C57BL/6J mice (Jackson Laboratory) were isolated. When comparing FRET response between WT and β1KO (Devic et al., 2001), all cells were isolated from 8–10-wk-old mice on a Friend leukemia virus B background. For trials using diabetic cardiomyocytes, cells were isolated from C57BL/6J mice that were fed either a high-fat diet (HFD; 60% fat; Research Diets; D12492J) for 5–6 mo until they developed diabetic cardiomyopathy or normal chow diet (10% fat; Research Diets; D12450J) as control for the same length of time (Wang et al., 2017).

The primary isolation method implemented for mouse cardiomyocytes has been previously described (Zhou et al., 2000). Mice were injected with 5,000 units/kg heparin (Fresenius Kabi) and anesthetized in 2–5% isoflurane, and hearts were excised and placed in a bath of ice-cold perfusion buffer (120 mM NaCl, 5.4 mM KCl, 1.2 mM NaH$_2$PO$_4$, 20 mM NaHCO$_3$, 1.2 mM MgSO$_4$, 5.6 mM glucose, 10 mM 2,3-butanedione monoxime [BDM], and 20 mM taurine, pH 7.34, bubbled with carbagen [Airgas] for 10 min, 0.22-μm filtered). The aorta was cannulated onto a 22-gauge gavage needle with a 1.2-mm ball (VWR) and transferred onto the perfusion apparatus (Radnoti) with buffer perfused at a constant flow rate of 7 drops/10 s by a Masterflex C/L (Cole Parmer). An Isotemp Circulator/Bath (Thermo Fisher Scientific) maintained the perfusate at a temperature of 37°C. The heart was predigested with 15 ml perfusion buffer containing 2.5 mg collagenase II (Worthington), 0.5 mg protease XIV, and 0.1% BSA. The heart was then digested with 20 ml perfusion buffer containing 10 mg collagenase II, 2 mg protease XIV, 0.1% BSA, and 50 μM CaCl$_2$, which was recirculated through the system until the heart was digested, as determined by touch. The heart was cut below the atria into a dish containing 5 ml digestion buffer and dissociated using forceps. The supernatant was placed in 5 ml stop buffer (12.5 μM CaCl$_2$ and 10% FBS in perfusion buffer) and was centrifuged at 500 rpm for 1 min. Remaining particles of tissue were further digested with 5 ml digestion buffer for 5 min at 37°C twice more to ensure maximal yield of cells. Succeeding steps were followed in each digestion sample in tandem. Cell pellets were resuspended and recovered in a gradient of calcium buffers to a concentration of 1 mM.

The second method for isolating cells was reported previously for use in preparation of cardiomyocytes for FRET analysis and uses gravity-fed pressure for perfusion (Lomas et al., 2015). Mice were injected with 5,000 units/kg heparin and anesthetized in 2–5% isoflurane. The aorta was clipped and cannulated onto a 22-gauge gavage needle with a 1.2-mm ball attached to a 1-ml syringe containing Tyrode buffer (130.0 mM NaCl, 5.6 mM KCl, 3.5 mM MgCl$_2$, 5.0 mM HEPES, 10.0 mM glucose, 20.0 mM taurine, and 0.4 mM Na$_2$HPO$_4$, pH 7.4, 0.22-μm filtered), and the needle was transferred onto the perfusion apparatus with buffer perfusion administered by gravity-fed pressure. An Isotemp Circulator/Bath attached to the perfusion apparatus maintained the perfusate at a temperature of 37°C. Once Tyrode solution was perfusing through the heart at a constant rate, the buffer was switched to Tyrode buffer containing 0.5 mg/ml collagenase II, 0.1 mg/ml protease XIV, 0.1% BSA, and 100 μM CaCl$_2$. Digestion was stopped when the drip rate dramatically increased. The heart was cut below the atria into a dish containing 5 ml digestion buffer and
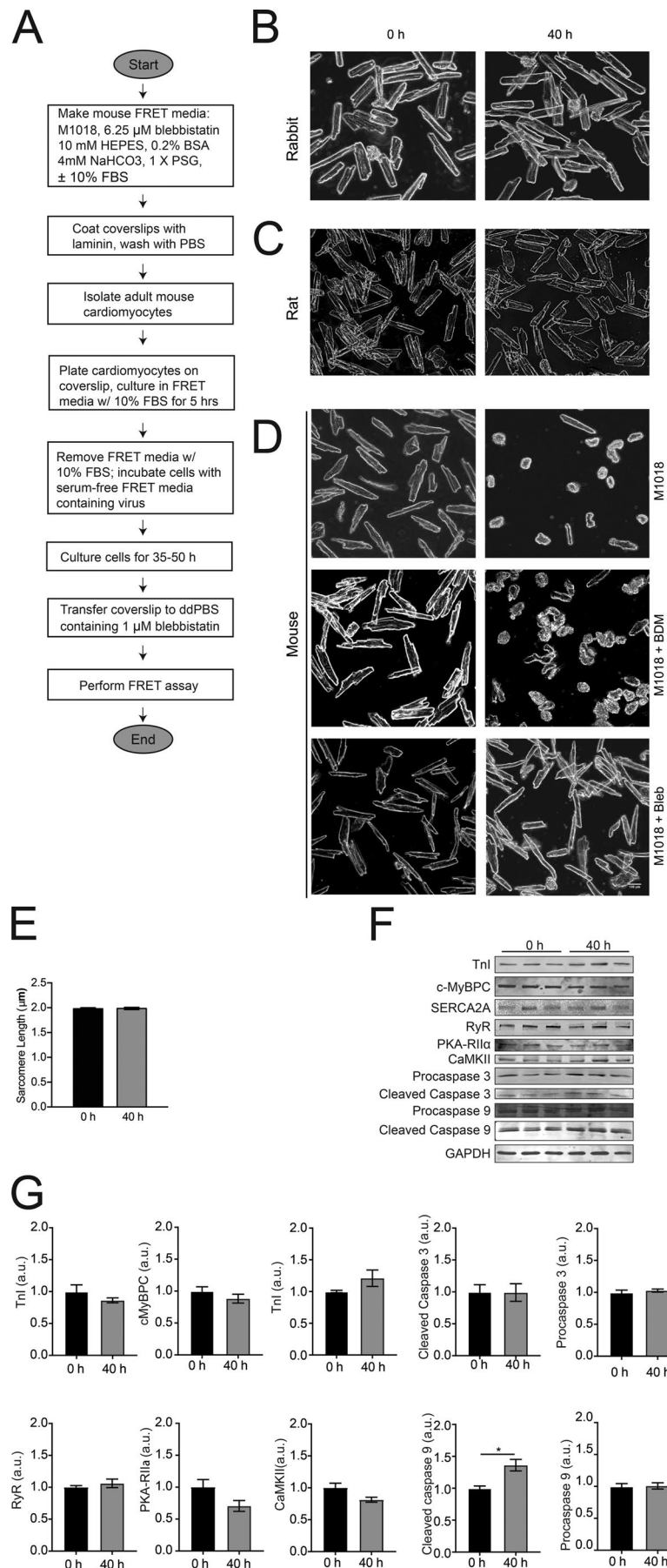
Reddy et al.
Optimization of FRET in mouse adult cardiomyocytes

Journal of General Physiology
https://doi.org/10.1085/jgp.201812119

1568

Figure 1. Morphology of adult cardiomyocytes from mouse, rat, and rabbit in different culturing conditions. (A) Flow chart of workflow for performing FRET assay on adult mouse cardiomyocytes. **(B)** Bright-field images of adult rabbit cardiomyocytes at 0- and 40-h time points that were maintained in DMEM. **(C)** Bright-field images of adult rat cardiomyocytes at 0- and 40-h time points that were maintained in M1018 containing 10 mM BDM. **(D)** Bright-field images of adult mouse cardiomyocytes at 0- and 40-h time points maintained in M1018 alone, M1018 with 10 mM BDM, or M1018 with 25 µM blebbistatin. All the bright-field images were captured at 20× magnification. Scale bar = 100 µm. **(E)** Sarcomere length measurements of cardiomyocytes at the normal time of infection (0 h) and 40 h later. **(F and G)** Western blot scans (F) and analysis (G) at the normal time of infection (0 h) and 40 h later of proteins important in proper functionality of cardiomyocytes. PKA RIIα, protein kinase A regulatory subunit IIα; SERCA2A, sarcoplasmic-endoplasmic reticulum calcium ATPase 2A. *, $P \leq 0.05$ by unpaired t test. Error bars represent ±SEM.

dissociated using forceps and 30 s of trituration with a 3-ml transfer pipette. 5 ml stop buffer (Tyrode buffer containing 1% BSA) was added, and the solution was filtered through 250-μm mesh. The suspension was centrifuged at 500 rpm for 1 min. Cells were resuspended and recovered in a gradient of calcium buffers to a concentration of 1 mM.

A third method for mouse cardiomyocyte isolation that has been previously described (Jian et al., 2016) was implemented to determine whether a pressure monitor in combination with using KCl as the sole inhibitor of heart beating would produce better cell quality for FRET than the above two methods. Mice were injected with 5,000 units/kg heparin and anesthetized in 2–5% isoflurane. Perfusion buffer (113 mM NaCl, 4.7 mM KCl, 1.2 mM $MgSO_4$, 0.6 mM Na_2HPO_4, 0.6 mM KH_2PO_4, 12 mM $NaHCO_3$, 10 mM $KHCO_3$, 10 mM HEPES, and 5 mM glucose, pH 7.4, 0.22-μm filtered) was injected into the femoral artery to arrest heart contraction. The aorta was clipped and cannulated onto a 22-gauge gavage needle with a 1.2-mm ball. The heart was excised from the chest, and the needle was transferred onto the perfusion apparatus with buffer perfusion administered by the Masterflex C/L. The flow rate was adjusted to maintain a pressure of 50–70 mmHg, which was measured using a BLPR2 pressure transducer (WPI) and SYS-BP1 pressure monitor (WPI). Perfusate temperature was maintained at 37°C by an Isotemp Circulator/Bath. After the perfusate was clear of blood, the system was switched to 50 ml digestion solution (300 units/ml collagenase II, 0.04 mg/ml protease XIV, and 12.5 μM $CaCl_2$ in perfusion buffer). The pump rate was adjusted continually to maintain a constant pressure between 50 and 70 mmHg until there was a dramatic drop in pressure to ~30 mmHg. The heart was cut below the atria into a dish containing 30 ml stop buffer (10% FBS and 12.5 μM $CaCl_2$ in perfusion buffer) and was dissociated using forceps and 30 s of trituration with a 3-ml transfer pipette. The suspension was filtered through a 250-μm mesh and centrifuged at 500 rpm for 1 min. Cells were resuspended and recovered in a gradient of calcium buffers to a concentration of 1 mM.

The isolation procedure for Zucker rat adult cardiomyocytes has been previously reported (Zhou et al., 2000). In essence, the same procedure was performed for rat isolation as was indicated in the primary protocol for mouse isolation, with the following modifications. The heart was cannulated onto a blunted 17-gauge needle (VWR); predigested with 30 ml perfusion buffer containing 5.0 mg of collagenase II, 1.0 mg protease XIV, and 0.1% BSA; and digested with 40 ml perfusion buffer containing 20 mg collagenase II, 4 mg protease XIV, 0.1% BSA, and 50 μM $CaCl_2$. The heart was cut into a dish containing 10 ml digestion buffer, and the supernatant was placed in 10 ml stop buffer (12.5 μM $CaCl_2$ and 10% FBS in perfusion buffer).

New Zealand white rabbit cardiomyocytes were isolated as previously described (Madhvani et al., 2011). Rabbits were anesthetized with 5% isoflurane and injected with 5,000 units/kg heparin before the heart was excised. Hearts were placed in an ice-cold bath of perfusion solution (138 mM NaCl, 5.4 mM KCl, 1 mM $MgCl_2$, 0.33 mM NaH_2PO_4, 10 mM $NaHCO_3$, 2 mM glucose, 10 mM HEPES, 2.5 mM pyruvic acid, and 10 units/L insulin, pH 7.4, 0.22 μm filtered) containing 1 mg/ml BSA and cannulated onto a Tygon tubing connector (Radnoti). The Tygon tubing con-

nector was transferred onto the perfusion apparatus with buffer perfusion administered by the Masterflex C/L until the perfusate was clear of blood while an Isotemp Circulator/Bath maintained the perfusate temperature at 37°C. The heart was then digested with 150 ml perfusion buffer containing 150 mg collagenase II and 8 mg protease XIV which was recirculated through the system until the heart was digested, as determined by touch. The heart was cut below the atria into a dish containing perfusion buffer with BSA, cut into pieces, and triturated for 30 s with a 3-ml transfer pipette. The resulting suspension was filtered through a 250-μm mesh and centrifuged at 500 rpm for 1 min. The cell pellet was resuspended and recovered in a gradient of calcium buffers to a concentration of 1 mM.

Cardiomyocyte culture conditions
M1018 was made according to the manufacturer's directions, using cell culture–grade $NaHCO_3$ and penicillin-streptomycin-glutamate (Mediatech). Medium was further supplemented, as indicated, with 10 mM BDM, 0.5 μM cytochalasin D, 10 mM HEPES, 0.2% BSA, 10% FBS, 5 mM taurine, and/or 1× insulin-transferrin-selenium (ITS; Thermo Fisher Scientific). pH was adjusted to 7.35 or 7.8 using NaOH (Thermo Fisher Scientific) and HCl (Thermo Fisher Scientific). All media were 0.22-μm sterile filtered before use. (-)-Blebbistatin (Cayman) or (S)-nitro-blebbistatin (Cayman) was dissolved to a concentration of 25 mM in filtered, cell culture–grade DMSO before being further diluted, as indicated, into the medium.

Cell culturing and infection
#0 glass coverslips (Karl Hecht) were coated in laminin (Life Technologies). Laminin was diluted 100× in sterile-filtered ddPBS (137 mM NaCl, 2.7 mM KCl, 10 mM Na_2HPO_4, and 1.8 mM KH_2PO_4, pH 7.4). 100 μl of the diluted laminin was placed on each coverslip, which was placed in a 37°C incubator with 5% carbon dioxide for a minimum of 2 h. Coverslips were moved to 24-well plate wells (Falcon) and washed three times with sterile-filtered ddPBS.

For most cultures, 20,000 cells were plated per each laminin-coated #0 glass coverslip in a 24-well plate in 500 μl of 10% serum-containing medium for 5 h in a 37°C incubator with 5% carbon dioxide. Medium was then replaced with 500 μl serum-free medium containing virus coding for the specified FRET biosensor and then placed at 37°C with 5% carbon dioxide. For cultures using the previously reported cytochalasin D–containing medium (Lomas et al., 2015), 20,000 cells were plated in 500 μl of 2.5% serum-containing medium for 2 h, switched to serum-free medium containing the virus for 3 h, and then switched to serum-free medium containing 0.5 μM cytochalasin D for 25 h. The AKAR3, Epac-S[H187] (Epac-based sensor #H187), ICUE3 (indicator of cAMP using Epac 3), Camui, and cGi500 sensors have all been previously described (Takao et al., 2005; Allen and Zhang, 2006; Russwurm et al., 2007; DiPilato and Zhang, 2009; Klarenbeek et al., 2015). Viruses were produced using the AdEasy system (Luo et al., 2007; Qbiogene). 95–99% of cells were infected within each experiment.

Microscope image acquisition
At the specified time points after infection, the medium was changed to serum-free medium without virus. The glass coverslip was transferred to a glass-bottom culture dish (MatTek)

containing 3 ml room temperature ddPBS. For cells cultured in blebbistatin-containing medium, the ddPBS was also supplemented fresh daily with 1 µM blebbistatin.

A Zeiss AXIO Observer A1 inverted fluorescence microscope equipped with a Hamamatsu Orca-Flash 4.0 digital camera and controlled by Metaflor software (Molecular Devices) acquired phase-contrast, CFP480, and FRET images. Phase-contrast and CFP480 images were collected with 20× and 40× oil-immersion objective lenses, and FRET images were collected using a 40× oil-immersion objective lens. Images for FRET analysis were recorded by exciting the donor fluorophore at 430–455 nm and measuring emission fluorescence with two filters (475DF40 for cyan and 535DF25 for yellow). Background subtraction of each fluorophore channel was performed by measuring the intensity of signal in an area of the imaging dish that had no cells present and subtracting it from the values present in cells of that dish. Images were acquired every 30 s, with exposure time of 200 ms on each channel. The donor/acceptor FRET ratio was calculated and normalized to the ratio value of baseline. CFP images were acquired by exciting the donor fluorophore at 430–455 nm and measuring emission fluorescence with the 475DF40 filter for 25 ms. Phase-contrast images were collected using a broad-spectrum incandescent light without filters for 25 ms.

Once cells normalized to UV exposure under FRET analysis conditions, an appropriate stimulant was added to the glass-bottom culture dish, and the change in FRET ratio was recorded. 10^{-5} M forskolin (IC Lab) + 10^{-4} M 3-isobutyl-1-methylxanthine (IBMX; Calbiochem) or 10^{-7} M isoproterenol were applied with AKAR3, ICUE3, and Epac-S^{H187}; 5×10^{-5} M sodium nitroprusside (SNP) was applied for cGi500; and 2×10^{-4} M CaCl$_2$ was applied for Camui. Average normalized curves and average maximal responses to stimulation were graphed based on FRET ratio changes.

Sarcomere length

Sarcomere length was measured as previously described (Jian et al., 2014). Freshly isolated adult mouse cardiomyocytes were placed on laminin-coated coverslips and incubated at 37°C and 5% carbon dioxide for 5 h in M1018 supplemented with 6.25 µM blebbistatin, 10 mM HEPES, 0.2% BSA, and 10% FBS. Medium was changed to serum-free medium of the same blend. Sarcomere length was then measured (0 h) and again measured 40 h later using an IonOptix system to implement a fast Fourier transform algorithm to estimate the light–dark striation pattern frequency in the cardiomyocyte. This striation pattern frequency, recorded in sarcomeres per pixel using a high-speed camera (MyoCam-S at 240–1,000 frames/s), was converted to sarcomere length by using a calibration slide with 2.5-µm increments (Edmund Industrial Optics UV Fused Silica Ronchi Slide, 400 lines/mm) to provide the software with a pixels-per-distance conversion factor. This conversion factor allowed for conversion from sarcomeres per pixel to distance per sarcomere.

Western blot

Adult mouse cardiomyocytes from a given mouse were plated in two laminin-coated 5-cm dishes at a concentration of 40,000 cells/ml in M1018 containing 6.25 µM blebbistatin, 10 mM HEPES, 0.2% BSA, and 10% FBS. Cells were incubated at 37°C for 5 h. The medium was then changed to serum-free medium of the same blend. One well was lysed with radioimmunoprecipitation assay buffer (25 mM Tris HCl, pH 7.6, 150 mM NaCl, 1% IGEPAL, 1% sodium deoxycholate, 0.1% SDS, and 1 mM EDTA containing protease and phosphatase inhibitors [100 mM Na$_3$F, 1 mM Na$_2$VO$_4$, 1 mM glycerol, 2.5 mM NaP$_2$O$_7$, 10 µg/ml leupeptin, 1 mM PMSF, and 10 µg/ml aprotinin]) at this time point, which is when viral infection for FRET experimentation normally takes place. The second well of cells from each mouse was lysed with radioimmunoprecipitation assay buffer (25 mM Tris HCl, pH 7.6, 150 mM NaCl, 1% IGEPAL, 1% sodium deoxycholate, 0.1% SDS, and 1 mM EDTA containing protease and phosphatase inhibitors [100 mM Na$_3$F, 1 mM Na$_2$VO$_4$, 1 mM glycerol, 2.5 mM NaP$_2$O$_7$, 10 µg/ml leupeptin, 1 mM PMSF, and 10 µg/ml aprotinin]) 40 h later, which is the time that FRET experimentation normally takes place. Total protein concentrations were normalized after bicinchoninic acid assay (Pierce) detection. Replicates from three mice were resolved simultaneously by SDS-PAGE on a 4–20% gradient gel and transferred to polyvinylidene fluoride membrane. Primary antibodies that were implemented for protein detection were troponin I (TnI; 4002; Cell Signaling), cardiac-specific myosin binding protein c (c-MyBPC; gift from S. Sadayappan, University of Cinicinnati, Cincinnati, OH; Sadayappan et al., 2006), sarcoplasmic-endoplasmic reticulum calcium ATPase 2A (SERCA2A; 2A7-A1; Thermo Fisher Scientific), RyR (34C; Thermo Fisher Scientific), protein kinase A regulatory subunit IIα (612243; BD), CaMKII (sc-5306; Santa Cruz), caspase 3 (Casp3; sc-2171759; Santa Cruz), caspase 9 (Casp9; sc-56076), and GAPDH (97166; Cell Signaling). Visualization was actualized with an Odyssey scanner (Li-Cor) after incubation in either antirabbit or antimouse IRDye 680CW or 800CW. Band intensities were quantified with ImageJ (NIH), divided by GAPDH values, and normalized to the average of the 0-h values.

Statistical analysis

All values are presented as mean ± SEM, and either unpaired t tests or one-way ANOVA with Bonferroni post hoc test was performed between mean values where indicated using GraphPad Prism 7.

Results

Blebbistatin preserves adult mouse cardiomyocyte morphology

Adult rabbit cardiomyocytes were cultured in DMEM, and adult rat cardiomyocytes were cultured in M1018 containing 10 mM BDM. As previously reported (Barbagallo et al., 2016), rabbit and rat cardiomyocytes retained rectangular morphology after 40 h of adenovirus infection (Fig. 1, B and C). Mouse cardiomyocytes were placed in similar culturing conditions, congruent with the methods reported by us and the Nikolaev group (Fig. 1 D; Soto et al., 2009; Börner et al., 2011; Wright et al., 2014). After 40 h, very few adult mouse cardiomyocytes in these cultures retained rectangular morphology. However, when the previously reported in vitro skeletal muscle myosin II K$_I$ concentration of 25 µM blebbistatin (Kovács et al., 2004) was included in the medium, the adult mouse cardiomyocytes retained normal morphology as

Reddy et al.
Optimization of FRET in mouse adult cardiomyocytes

Journal of General Physiology 1571
https://doi.org/10.1085/jgp.201812119

previously reported (Kabaeva et al., 2008). To further explore whether the cells cultured in the blebbistatin media had any discernable changes in the extended culture time, we measured sarcomere length and examined protein concentrations by Western blot. There was not a significant difference in sarcomere length between freshly isolated cells and cells cultured for 40 h, the normal time that the FRET assay is performed (Fig. 1 E). The sarcomere lengths were within previously measured length ranges for healthy mouse cardiomyocytes at rest (King et al., 2011). In addition, there were no significant changes to myofilament proteins (TnI and c-MyBPC), excitation contraction coupling proteins (SERCA2A and RyR), kinases (PKA-RIIα and CaMKII), and caspase 3, but there was a significant increase in caspase 9 at the 40-h time point (Fig. 1, F and G).

CFP images of cardiomyocytes 40 h after infection with the PKA biosensor AKAR3 were then captured to determine whether FRET would be possible. However, 25 µM blebbistatin and 0.05% DMSO yielded a large deposition of fluorescent spots that would make FRET practically impossible (Fig. 2 A). Increasing DMSO concentration to 0.1% had no effect on fluorescent deposition of blebbistatin (not depicted). Therefore, reduced concentrations of blebbistatin were attempted together with reduced DMSO concentrations. Reducing the blebbistatin concentration to 6.25 µM in 0.025% DMSO caused no difference in culture morphology while greatly reducing the fluorescent blebbistatin deposition (Fig. 2 A). When blebbistatin concentrations were further reduced, the morphology of the cultured cells suffered (Fig. 2 A) and the cells often shrank when exposed to UV light.

Although using 6.25 µM blebbistatin greatly reduced autofluorescent spotting to allow for reproducible FRET readings, we attempted to optimize the media conditions to further reduce autofluorescence and improve cell health. Other components present in previously published mouse cardiomyocyte media (Kabaeva et al., 2008; Ackers-Johnson et al., 2016) were supplemented in tandem with 6.25 µM blebbistatin to determine whether autofluorescence could be further reduced and whether cell culture quality could be further improved. Supplementing 10 mM HEPES further reduced autofluorescent spotting (Fig. 2 B). Supplementing 0.2% BSA improved cell attachment to the coverslip and reduced the number of cells that failed to maintain rod shape morphology when placed under UV light, but led to increases in autofluorescent spots (Fig. 2 B). When both HEPES and BSA were applied together, the number of autofluorescent spots was inconsequential (Fig. 2 B). Meanwhile, supplementing ITS or taurine to the media had no appreciable effect on the culture quality or autofluorescent spotting (not depicted). Using a medium with pH 7.8 rather than 7.35 had no appreciable improvement on the culture (not depicted). (S)-nitro-blebbistatin (Képiró et al., 2014; Várkuti et al., 2016) is a derivative of (-)-blebbistatin that is not fluorescent, does not break down in UV light, and does not produce reactive oxygen species and phototoxic byproducts like blebbistatin when exposed to UV light (Kolega, 2004; Sakamoto et al., 2005; Mikulich et al., 2012). 20 µM (S)-nitro-blebbistatin was supplemented to the media to determine whether the culture quality could be further improved. Cells were infected with AKAR3, and at the time of infection as well as at 40 h after infection, images were captured. There was no

significant difference in cell morphology in cells cultured in (S)-nitro-blebbistatin compared with cells from the same mice cultured in the presence of blebbistatin (Fig. 2, C and D).

Quality adult myocyte culture for optimal expression of PKA biosensors and FRET analysis

To determine how long mouse cardiomyocytes would retain rod-shape morphology in the newly characterized cell culture medium, an image was collected every 10 h after infection with the PKA biosensor AKAR3. Cardiomyocytes cultured in the same medium without blebbistatin were used as controls. Mouse adult myocytes in the culture medium with blebbistatin maintained a rectangular morphology for 50 h after infection. At 60 h after infection, cells became rounded on the edges (Fig. 3 A) and tended to shrink when exposed to UV light.

Adult mouse cardiomyocytes were cultured in medium containing cytochalasin D as previously reported, in comparison (Lomas et al., 2015). At the recommended 25-h time point, 10% of cells in the culture had retained rectangular morphology, but by 30 h, only very few cells retained this morphology (Fig. 3 B). FRET response was also tested 25 h after infection of AKAR3 in mouse adult myocytes cultured in the medium with cytochalasin D as previously reported (Lomas et al., 2015), which was compared with the FRET response of myocytes cultured with blebbistatin. Myocytes in both cultures displayed increases in FRET ratio after costimulation with forskolin and IBMX; however, the cells cultured in cytochalasin D had a significantly lower AKAR3 response than the cells cultured in blebbistatin (Fig. 3, C–E). Furthermore, the cells cultured in cytochalasin D tended to shrink when exposed to UV light, making it difficult to collect enough data points. In contrast, very few of the cells cultured in blebbistatin shrink when exposed to UV light at this time point. Overall, the cytochalasin D–containing medium worked poorly to maintain culture quality that is required for extensive analysis of signaling networks, while the newly developed blebbistatin-containing medium helped to maintain cell morphology well throughout the culture.

Because the blebbistatin-containing culture maintained signaling transduction ability at 25 h postinfection, later time points were then further explored to determine the optimal time for performing the FRET assay. Phase-contrast and CFP images of AKAR3 were collected at 0, 20, 30, 35, 40, 50, and 60 h after infection to optimize the expression of the biosensor for FRET analysis in mouse adult cardiomyocytes. Rabbit adult cardiomyocytes were used as control. A similar expression profile emerged from both mouse and rabbit cells (Fig. 4, A and B). To determine the time window in which reproducible FRET data can be collected, the FRET assay was performed 20, 30, 35, 40, 50, and 60 h after infection with AKAR3 by stimulating the cells with a mixture of forskolin and IBMX, which activate adenylyl cyclases and inhibit phosphodiesterases, respectively (Fig. 5, A–D). Compared with rabbit cardiomyocytes, adult mouse cardiomyocytes produced a peak reproducible response earlier, at 35 h postinfection. Responses were similar from 35 to 50 h in mouse cells. By the 60 h time point, mouse cardiomyocytes were unresponsive to stimuli, while rabbit cardiomyocytes were even more responsive (Fig. 5, A–D). We also determined how cells cultured in the nonfluores-
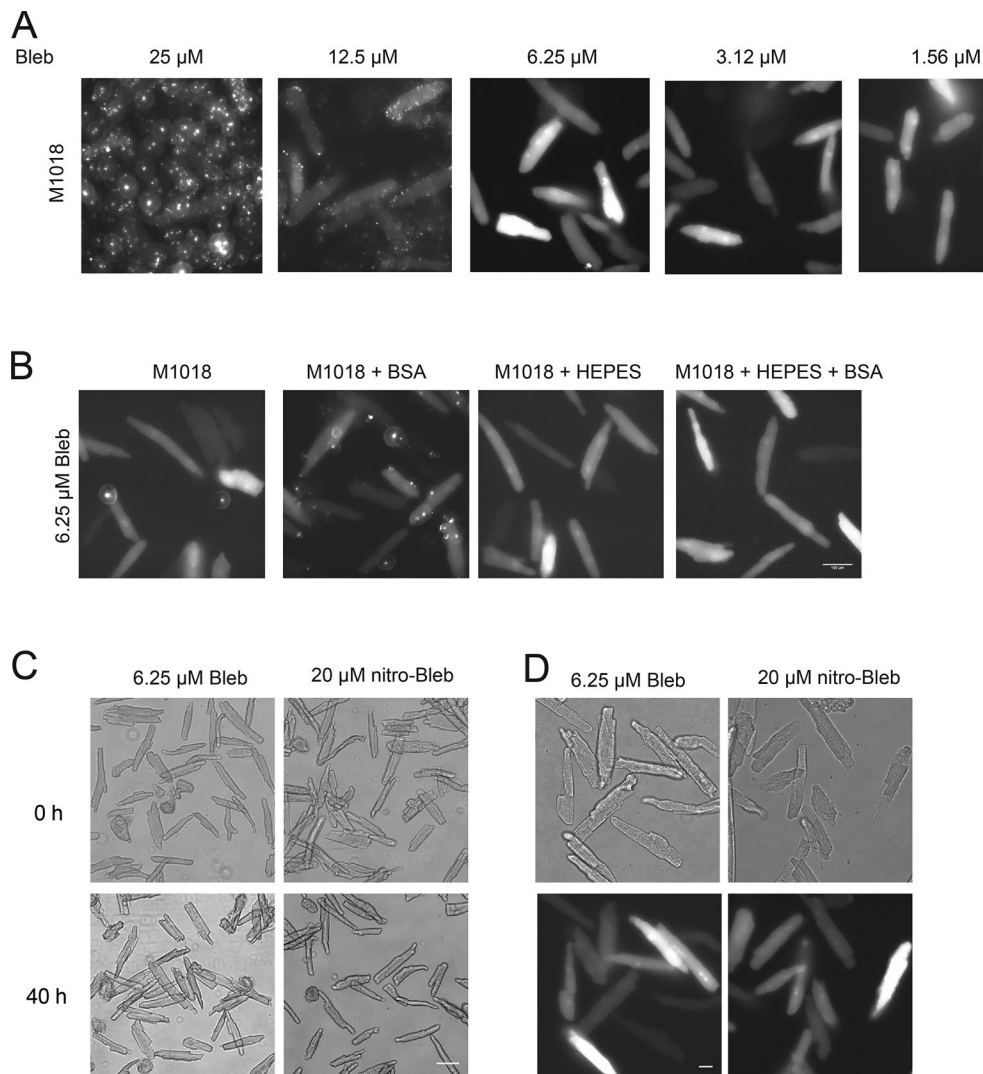
Figure 2. **Media optimization to eliminate autofluorescent properties in adult cardiomyocyte culture. (A)** CFP images of adult mouse cardiomyocytes 40 h after infection with the PKA FRET biosensor, AKAR3, maintained in M1018 with different doses of blebbistatin. Images were recorded at 40× magnification. Scale bar = 100 µm. **(B)** CFP images of adult mouse cardiomyocytes 40 h after infection with AKAR3 maintained in M1018 with 6.25 µM blebbistatin, 0.2% BSA, and 10 mM HEPES as indicated. Images were recorded at 40× magnification. Scale bar = 100 µm. **(C)** Bright-field images, recorded at 20× magnification at the time of infection (0 h) and 40 h later, of myocytes cultured in M1018 with 10 mM HEPES and 0.2% BSA, and either 6.25 µM blebbistatin or 20 µM (S)-nitro-blebbistatin. Scale bar = 100 µm. **(D)** Bright-field and CFP images collected at the time of infection (0 h) and 40 h later. Images were recorded at 40× magnification. Scale bar = 100 µm.

cent derivative, (S)-nitro-blebbistatin, would perform in FRET assays. FRET was performed on cells from the same animals cultured in media containing 20 µM (S)-nitro-blebbistatin 40 h after infection with AKAR3. There was no significant difference in FRET response in cells cultured in (S)-nitro-blebbistatin compared with those with blebbistatin (Fig. 5, E and F).

Translation of the FRET assays to varying myocyte isolation protocols, mouse models, and FRET-based biosensors
Assays that are commonly done using isolated adult cardiomyocytes, including patch-clamp experiments, require healthy cells with intact membrane structure that are free of substances such as BDM or taurine. There is also often debate about which isolation method needs to be performed for a given assay (Louch et al., 2011; Jian et al., 2016). We checked three isolation methods

to see whether our newly developed FRET assay was dependent on a specific isolation protocol, as was suggested in a previous study on mouse cardiomyocyte FRET (Lomas et al., 2015). Differences in the isolation methods included changes in the contents of the isolation buffer, changes in how the heart was excised and cannulated, and changes in how perfusion was regulated. The methods for isolation are detailed in the Materials and methods section. All three isolation methods had similar robust results for cell culture and AKAR3 FRET biosensor analysis (Table 1).

The proposed culturing method was also tested in adult mouse cardiomyocytes isolated from β1KO mice to show the proof of principle that the method is applicable to transgenic mouse cells. The data shown in Fig. 6 (A and B) demonstrate that adult β1KO cardiomyocytes have a similar response to cotreatment with forskolin and IBMX as WT cells but have a reduced response to
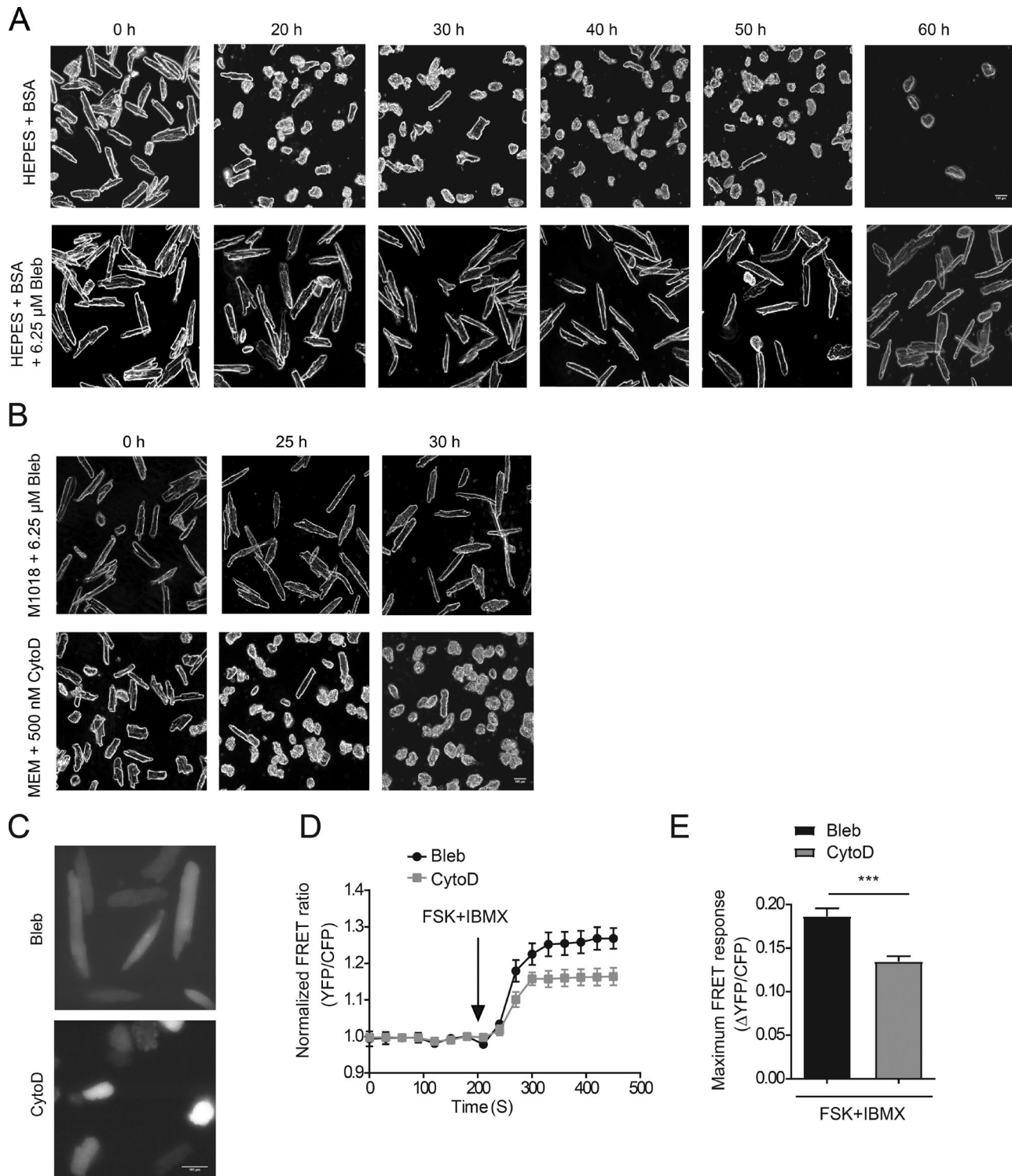
Figure 3. **Blebbistatin improves morphology of adult mouse cardiomyocytes during extended culture. (A)** Bright-field images of adult mouse cardiomyocytes every 10 h when cultured in M1018 + HEPES + BSA with or without 6.25 µM blebbistatin. **(B)** Bright-field images displaying the morphology of adult mouse cardiomyocytes at previously recommended time points with either 6.25 µM blebbistatin or 500 nM cytochalasin D in the medium. Bright-field images were photographed at 20× magnification. Scale bar = 100 µm. **(C)** CFP images of adult mouse cardiomyocytes 25 h after infection with AKAR3 when cultured in medium containing either 6.25 µM blebbistatin or 500 nM cytochalasin D. CFP images were collected at 40× magnification. Scale bar = 100 µm. **(D and E)** Mouse myocytes cultured with blebbistatin and cytochalasin D were costimulated with 10 µM forskolin (FSK) and 100 µM IBMX 25 h after infection with AKAR3 biosensor. The normalized FRET ratios over time are plotted as an average trace, and maximal increases in AKAR3 FRET ratio are depicted in the bar graph. ***, P ≤ 0.001 by unpaired *t* test. Error bars represent ±SEM.
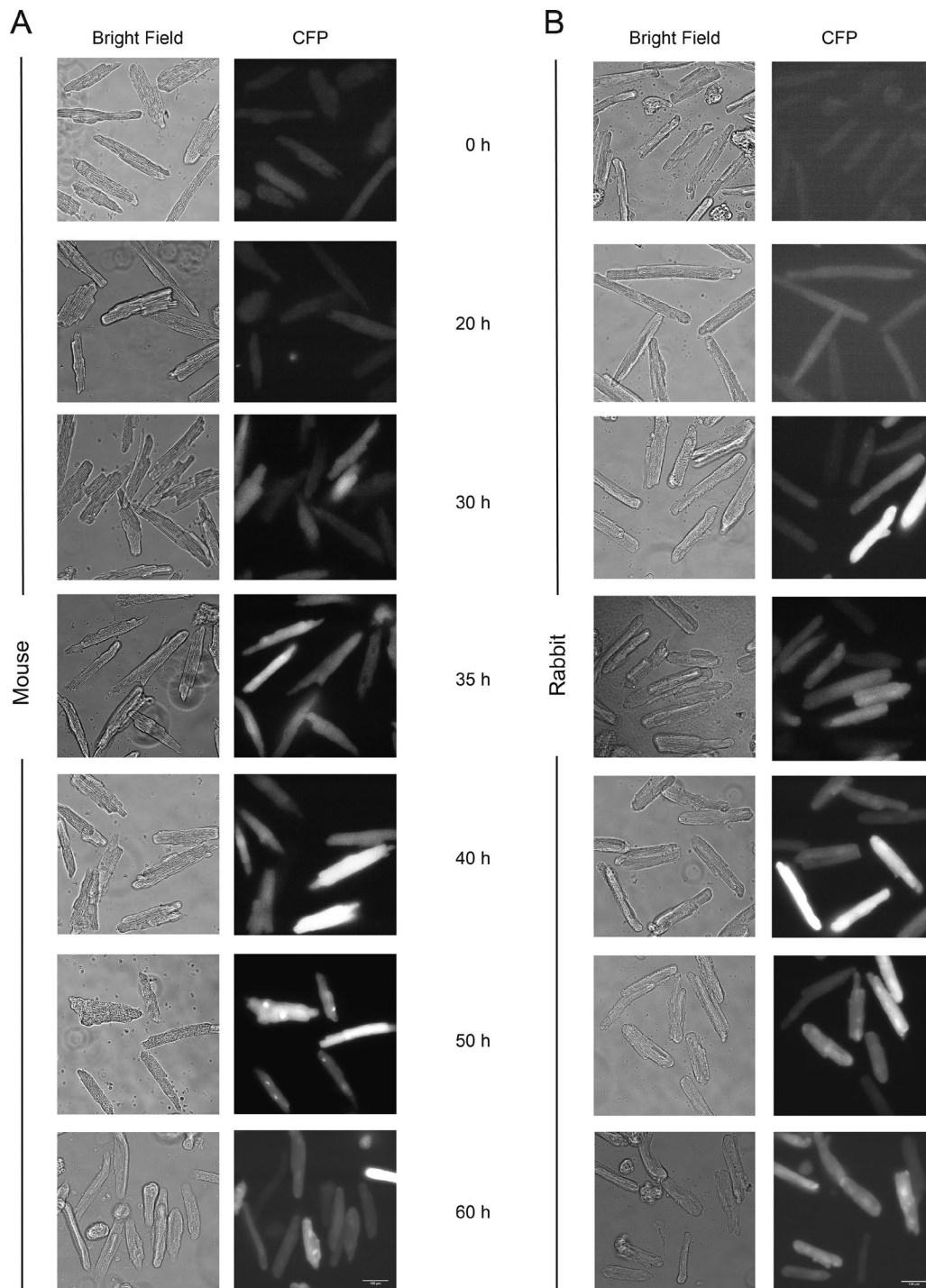
Figure 4. **Time-dependent expression of the PKA FRET biosensor, AKAR3, in adult mouse and rabbit cardiomyocytes. (A and B)** Bright-field and corresponding CFP fluorescence images of adult mouse (A) and rabbit (B) cardiomyocytes at different time points of culture as indicated. All images were acquired at 40× magnification. Scale bar = 100 µm.

isoproterenol, an agonist of β adrenergic receptors. Meanwhile, cardiomyocytes were also isolated from mice with diabetic cardiomyopathy after feeding with HFD to show that this method for FRET analysis is translatable to cardiac disease models. HFD cardiomyocytes displayed a reduced response to isoproterenol compared with cells from age-matched littermate controls fed with normal chow diet (Fig. 6, C and D). This observation indi-

cates that in pathological diabetic cardiomyocytes, the β-adrenergic response is impaired.

The newly developed culturing method was then tested with a variety of CFP/YFP-based biosensors. Isolated adult mouse cardiomyocytes were infected with the sensors cGi500 for cGMP, Camui for CaMKII, and ICUE3 and Epac-S[H187] for cAMP (Takao et al., 2005; Allen and Zhang, 2006; Russwurm et al., 2007; DiPilato
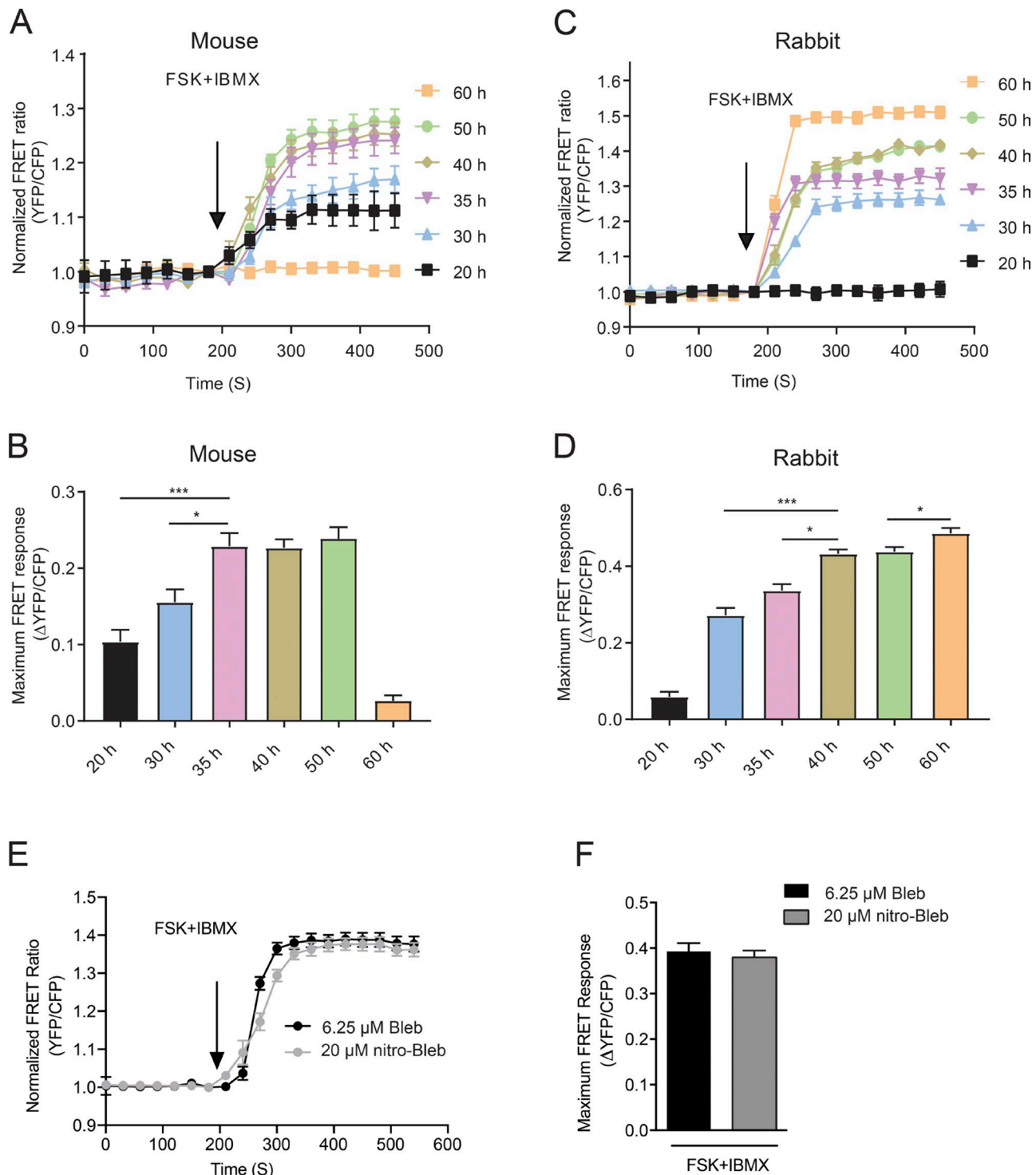
Figure 5. **Optimization of the expression time of AKAR3 for reproducible FRET measurements in adult cardiomyocytes. (A–D)** Adult mouse and rabbit cardiomyocytes expressing the PKA biosensor, AKAR3, were costimulated with 10 µM forskolin (FSK) and 100 µM IBMX. The traces depict time courses of changes in FRET ratio, and the maximal increases of FRET ratio are plotted in the bar graphs. *, P ≤ 0.05; ***, P ≤ 0.001 by one-way ANOVA followed by post hoc Bonferroni test. **(E)** WT mouse myocytes cultured in medium containing either 6.25 µM blebbistatin or 20 µM *(S)*-nitro-blebbistatin that were expressing the PKA biosensor, AKAR3, were stimulated with 10 µM FSK + 100 µM IBMX, and the average FRET ratios over time were plotted as a trace. **(F)** The average maximal increases in AKAR3 FRET ratio in myocytes from part E were plotted. Significance was calculated by unpaired *t* test. Error bars represent ±SEM.

and Zhang, 2009; Erickson et al., 2011; Klarenbeek et al., 2015). Both cGi500- and Camui-infected adult mouse cardiomyocytes showed a robust change in FRET ratio upon treatment with activators of the sensors from 35 to 50 h postinfection (Fig. 6, E,

F, and H). ICUE3-infected adult mouse cardiomyocytes, no matter the length of expression, never produced a robust change in FRET ratio when treated with forskolin combined with IBMX. The expression of ICUE3 was low, especially in the CFP channel

Table 1. **Isolation protocol comparison**

Procedure	Protocol 1	Protocol 2	Protocol 3
Buffer delivery	Constant flow by minipump	Gravity-induced flow	Constant pressure monitored and adjusted by minipump
Cannulation	Excision, then cannulation	In-chest cannulation	In-chest cannulation
Buffer contents	NaCl, KCl, NaH$_2$PO$_4$, NaHCO$_3$, MgSO$_4$, glucose, BDM, taurine	NaCl, KCl, MgCl$_2$, HEPES, glucose, taurine, Na$_2$HPO$_4$	NaCl, KCl, MgSO$_4$, Na$_2$HPO$_4$, KH$_2$PO$_4$, NaHCO$_3$, KHCO$_3$, HEPES, glucose
Isolation initial survivorship rate	49–54% rod shaped	73–83% rod shaped	80–90% rod shaped
Basal CFP/YFP ratio (a.u.)	0.9925–1.0051	0.9957–1.0012	0.9802–0.9972
Normalized 40 h AKAR3 FRET Ratio change (a.u.)	1.245–1.2514	1.236–1.2416	1.267–1.2692

(not depicted). In comparison, the recently developed cAMP sensor, Epac-S^{H187} (Klarenbeek et al., 2015), displayed robust changes in FRET ratio in adult mouse cardiomyocytes 30–40 h after infection upon stimulation with forskolin and IBMX combined (Fig. 6, G and H). Table 2 details optimal expression and experimental windows of individual biosensors in adult mouse cardiomyocytes.

Discussion

In this study, a new cell culturing protocol for adult mouse cardiomyocytes was developed that allows for exploration of intracellular signaling transduction using FRET-based biosensors through adenoviral-mediated expression. This method is highly adaptable to a variety of isolation techniques, which is a major point of concern in many other types of live cardiomyocyte assays such as patch-clamp experiments (Louch et al., 2011; Jian et al., 2016). Application of this method will allow a variety of genetic and pathological mouse models to be used to determine on a single-cell, time-dependent basis how signaling cascades in cardiomyocytes operate. Data presented in this paper show that the culturing method allows for transgenic and diseased mouse cardiomyocytes to be assayed with FRET techniques in similar fashion to normal WT cells. The culturing method presented here simplifies investigation of mouse cardiomyocyte signaling networks, as there is no need for complicated breeding schemes to cross transgenic biosensor-expressing mice with other genetic mouse models. Future implementation of this method in laboratories which use a diverse set of isolation techniques will allow a variety of genetic mouse models to be used to determine on a single-cell, time-dependent basis how signaling cascades in cardiomyocytes operate.

The main component in the media that improves culture conditions is blebbistatin. Previous research done on how to culture adult mouse cardiomyocytes for long-term studies shows that a culture medium containing blebbistatin improves short-term morphology and long-term survivorship (Kabaeva et al., 2008). Blebbistatin is a small molecule that selectively inhibits myosin II ATPase activity in an uncompetitive manner with the actin-detached state, which leads to relaxation of myofibrils in contractile cells (Kovács et al., 2004). Data presented in this paper shows that blebbistatin is superior over another reported myosin II inhibitor, BDM, in maintaining mouse myocyte morphology during extended culture in vitro to accommodate the expression of biosensors for FRET assays. This is probably because BDM also removes phosphate groups off other cytosolic proteins (Ostap, 2002) and causes mitochondrial dysfunction in cardiomyocytes by acting directly on the electron transport chain (Hall and Hausenloy, 2016). Conversely, blebbistatin has fewer off-target affects and minimal disturbance to mitochondrial health in cardiomyocytes (Hall and Hausenloy, 2016). Therefore, it is recommended that BDM be avoided for mouse cardiomyocyte culture and blebbistatin be used instead.

Blebbistatin has an in vitro K_i of 25 µM with myosin II in the nucleotide-free form and a similar K_i of 24 µM with the holoenzyme (Kovács et al., 2004). Using blebbistatin can therefore decrease ATP usage by up to 10 times (Kovács et al., 2004), extending the life of cells by saving energy reserves. But blebbistatin is autofluorescent (Swift et al., 2012), making it a difficult substance to work with when performing fluorescence imaging. Reducing the blebbistatin concentration to below the holo- and apo-enzyme K_i, at a concentration of 6.25 µM, still effectively protects cell morphology, sarcomere length, and protein expression levels in isolated cultures for the extended culture time needed for expression of FRET biosensors. Cell morphology and biochemistry may be protected at this low blebbistatin concentration because blebbistatin has high affinity with an intermediate state of nucleotide-bound myosin during its ATPase activity, with a measured K_M of 3.1 µM (Kovács et al., 2004). Low blebbistatin concentration allows for a reduction in the amount of autofluorescence, which enables FRET to be performed for a 10–15-h window without excessive damage to cell morphology.

Blebbistatin is unstable in blue-UV light and has been reported to produce reactive oxygen species and phototoxic byproducts when it breaks down (Kolega, 2004; Sakamoto et al., 2005; Mikulich et al., 2012). One of the nonfluorescent derivatives, (S)-nitro-blebbistatin (Képiró et al., 2014; Várkuti et al., 2016), was supplemented into the culture media instead of blebbistatin. When cells cultured in (S))-nitro-blebbistatin were tested side by side with cells cultured in blebbistatin, no discernable difference in morphology or FRET response was observed. Therefore, (S)-nitro-blebbistatin can be used as an alternative if experimentation with blebbistatin results in unmanageable fluorescence spots and/or myocyte cytotoxicity.
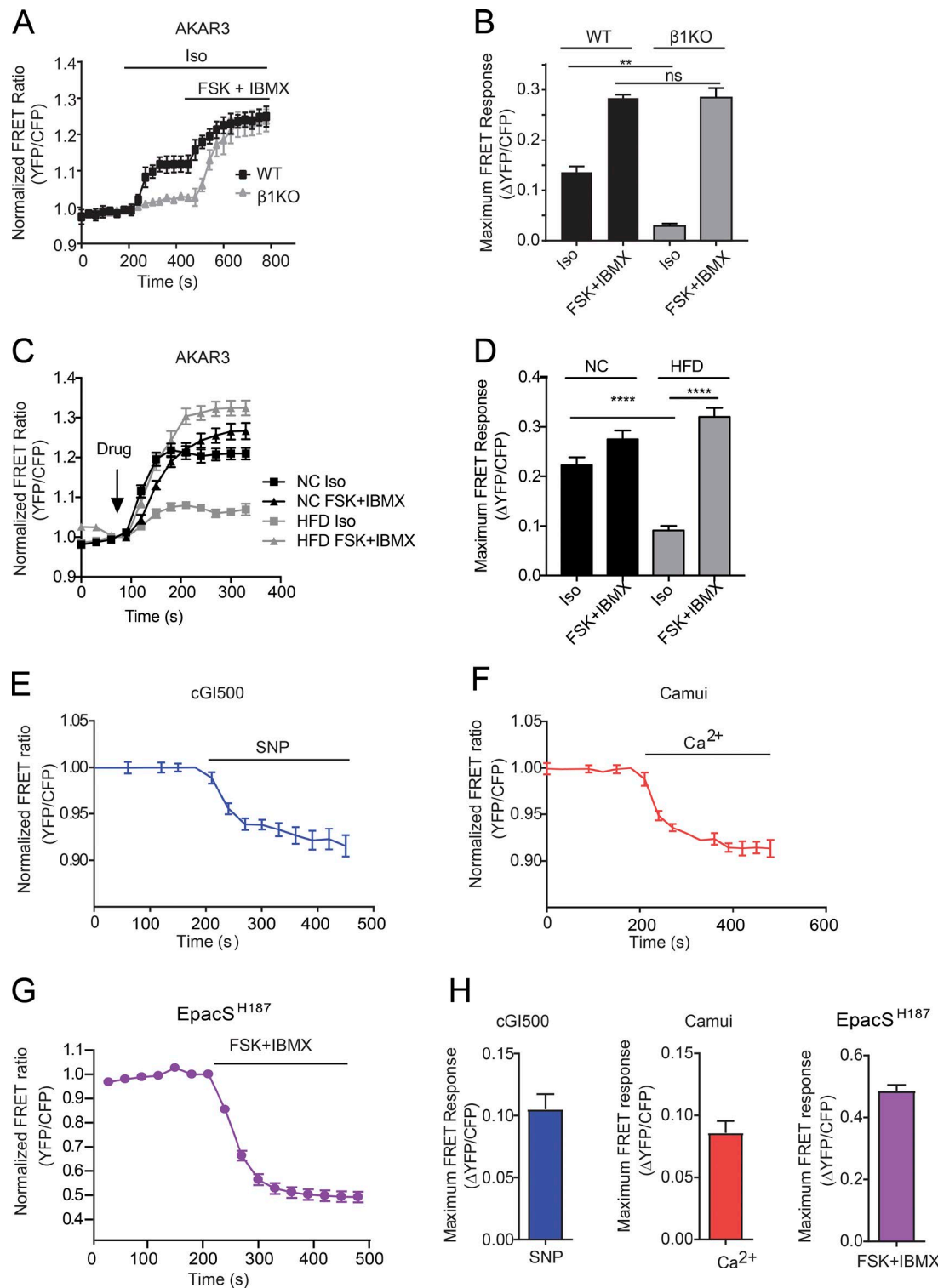
Figure 6. **Application of FRET measurements in transgenic adult mouse cardiomyocytes and with a variety of FRET biosensors. (A)** WT and β1KO mouse myocytes expressing the PKA biosensor, AKAR3, were stimulated with 100 nM isoproterenol (ISO) followed by 10 μM FSK + 100 μM IBMX, and the average FRET ratios over time were plotted as a trace. **(B)** The average maximal increases in AKAR3 FRET ratio in WT and β1KO myocytes were plotted. **, $P \leq 0.01$ by one-way ANOVA followed by post hoc Bonferroni test. **(C)** Normal chow (NC) and HFD mouse myocytes expressing the PKA biosensor, AKAR3, were stimulated with 100 nM isoproterenol (ISO) or 10 μM FSK + 100 μM IBMX; the average FRET ratios over time were plotted as a trace. **(D)** The average maximal increases in AKAR3 FRET ratio in NC and HFD myocytes were plotted. ****, $P \leq 0.0001$ by one-way ANOVA followed by post hoc Bonferroni test. **(E)** Adult mouse cardiomyocytes expressing the cGMP biosensor, cGI500, for 45–46 h were stimulated with 50 μM SNP. FRET ratio is plotted over time. **(F)** Adult mouse cardiomyocytes expressing the CaMKII biosensor, Camui, for 45–46 h were stimulated with 200 μM Ca^{2+}. FRET ratio is plotted over time. **(G)** Adult mouse cardiomyocytes expressing the cAMP biosensor, EpacS[H187], for 35–36 h were stimulated with 10 μM FSK + 100 μM IBMX. FRET ratio is plotted over time. **(H)** The average maximal changes in FRET ratio from E, F, and G are graphed. Error bars represent ±SEM.

Table 2.   **FRET sensor expression in adult mouse cardiomyocytes**

FRET probe	Citation	Full name	Detects	Donor	Acceptor	Linker	FRET time window (h)	Basal YFP intensity (a.u.)	Basal CFP intensity (a.u.)	Maximum YFP intensity (a.u.)	Maximum CFP intensity (a.u.)
AKAR3	Allen and Zhang, 2006	A kinase activity reporter 3	PKA activity	eCFP	Tandem cp^{173}Venus pair	Binding domain from kemptide and substrate domain from 14-3-3, with a 14-aa sequence in between	35–50	980–1,010	313–330	1,049–1,080	255–265
cGi500	Russwurm et al., 2007	cGMP indicator-500 nM	[cGMP]	eCFP	eYFP	Cyclic nucleotide monophosphate binding domains A and B from PKG (Gln^{79}-Tyr^{345})	35–50	3,803–3,901	1,049–1,101	3,471–3,207	1,143–1,208
Camui	Takao et al., 2005	Camui	CaMKII activity	CFP-S175G	Venus	Rat CaMKIIα	35–50	5,366–5,410	1,561–1,610	5,140–5,190	1,655–1,701
ICUE3	DiPilato and Zhang, 2009	Indicator of cAMP using Epac	[cAMP]	eCFP	Tandem cp^{194}Venus pair	Epac1	n/a	2,108–2,210	660–810	2,120–2,209	659–808
Epac-S^{H187}	Klarenbeek et al., 2015	Epac-based sensor #H187	[cAMP]	mTurquoise2	Tandem cp^{173}Venus pair	Catalytically dead Epac1 with deletion of the membrane targeting sequence and a point mutation of Q270E	30–40	1,624–1,709	246–260	1,186–1,198	353–369

Meanwhile, HEPES and BSA were added in an attempt to further eliminate fluorescence spots of blebbistatin. 10 mM HEPES and 0.2% BSA were effective at reducing precipitation of blebbistatin on the coverslips. HEPES is a Good's buffer zwitterion, which has been previously implemented in cultures of adult mouse cardiomyocytes (Kabaeva et al., 2008; Ackers-Johnson et al., 2016). HEPES can interact with compounds and proteins in solution in a way that allows them to stay biochemically available and soluble (Good et al., 1966; Sledź et al., 2010). HEPES may interact with blebbistatin in a similar fashion to prevent precipitation. BSA's main biological function is to keep a wide variety of substances soluble and buffered in blood (Francis, 2010), and BSA has been previously supplemented in cardiomyocyte culture media (Kabaeva et al., 2008; Ackers-Johnson et al., 2016). Interestingly, 0.2% BSA supplemented by itself increases the fluorescence spotting on the coverslips, but it improves cell attachment and health in culture and reduces the number of cells that shrink when placed under UV light. BSA also biologically acts as an antioxidant, stabilizes enzymes and biomolecules, and buffers ions in the media (Francis, 2010), which may be the mechanisms by which the BSA improves cell quality in these culturing conditions. Together, it is recommended that both be supplemented for culturing adult mouse myocytes for FRET. In addition, ITS and taurine, respectively, were tested in the media, but no improvement in culture quality was observed. Insulin can greatly change cellular metabolism, while taurine physiologically modifies calcium ion channel activity in the heart (Schaffer et al., 2010). Because many models of heart disease include changes in metabolism (Riehle and Abel, 2016) and calcium ion channel activity (Bers, 2008) and no improvement in the cell quality was observed, it is inadvisable to use insulin and taurine in cell cultures for FRET studies in adult mouse cardiomyocytes.

The implementation of the formulated adult mouse myocyte medium has allowed for FRET assays to be enacted with a variety of FRET biosensors including the PKA biosensor AKAR3, the cAMP biosensor Epac-S^{H187}, the CaMKII biosensor Camui, and the cGMP biosensor cGi500. Although the optimized blebbistatin-containing medium improves cell morphology, reduces autofluorescent spots, and curtails cell shrinking under UV light, there is a limit to how long cells can remain viable for the FRET assay. We found that the optimal time, with any sensor, that the adult cardiomyocytes were responsive in FRET assays was 35–50 h after infection. After 50 h, the cells often shrink under UV light. Those cells that do not shrink respond poorly to stimuli. There was an increase in cleaved caspase 9 at the 40-h time point, which may explain why cells tended to shrink at later time points, as active caspase 9 may be associated with cell shrinkage (Zimmermann et al., 2001). Meanwhile, the expression of biosensors also affects the optimal windows to measure the cell response: too low of expression yields high noise-to-signal ratio whereas high fluorescence intensity interferes with the FRET response after stimulation. For example, PKA biosensors still gave

responses at the 50-h time point, whereas CaMKII biosensors became unresponsive much sooner. Hence, both cell health and biosensor design affect the time window at which FRET assays can be performed.

Despite that this diverse array of CFP/YFP sensors are effective in this method, not all sensors attempted were equally efficacious. Although the fourth-generation cAMP sensor, Epac-S^{H187}, worked well, the third-generation cAMP sensor, ICUE3, did not, which is probably because of the different designs of the sensors. ICUE3 is based on the full length of exchange protein directly activated by cAMP (Epac); the membrane targeting sequence on Epac may make the endoplasmic reticulum expression and processing of the ICUE3 biosensor difficult, resulting in a low expression level in adult myocytes. In contrast, Epac-S^{H187} incorporates very bright and highly photobleach-resistant donor and acceptor, as well as a smaller linker composed of Epac with the membrane targeting sequence removed and a point mutation that increases the calcium affinity by 2.5-fold (Klarenbeek et al., 2015). Therefore, Epac-S^{H187} allows stronger and brighter sensor expression to detect cAMP dynamics in adult cardiomyocytes 30–40 h after infection. The data from cells expressing the cGi500 biosensor for cGMP display a clear response to cotreatment with forskolin and IBMX, but the change in FRET ratio was small. cGi500 has an EC$_{50}$ for cGMP of 500 µM (Russwurm et al., 2007), which is probably not optimized to detection of cGMP concentrations induced by neurohormonal stimuli. Another cGMP biosensor, red-cGES-DE5, has an EC$_{50}$ of ~40 nM (Nikolaev et al., 2006; Bork and Nikolaev, 2018) and could be used to detect small changes in cGMP concentration that are often present in cardiomyocytes.

In the future, implementation of this method with other biosensors, including biosensors localized to certain locations in the cell and combined with the new scanning ion conductance microscopy/FRET technology (Wright et al., 2014; Bazzazi et al., 2015; Barbagallo et al., 2016; Surdo et al., 2017) will be useful in determining the spatiotemporal dynamics of signaling cascades in cardiomyocytes. When applying FRET analysis with localized biosensors, it is important to consider how different compartments of the cell might be affected by blebbistatin. For example, one should remain cautious when measuring signal transduction with FRET biosensors targeted onto the myofilaments (Barbagallo et al., 2016), because blebbistatin inhibits myosin II and can decrease rigid actin-myosin cross-bridge formation (Kovács et al., 2004). Modeling studies suggest that decreases in cross-bridge formation can lead to decreases in troponin calcium sensitivity (Sich et al., 2010), but studies in permeabilized mouse cardiac fibers and skinned rat trabeculae suggest that blebbistatin-inhibited cells have no change in calcium dynamics compared with uninhibited cells, although contractility is inhibited (Dou et al., 2007; Farman et al., 2008). Future study using targeted FRET biosensors in larger species' cardiomyocytes may also be able to shed light on alterations that blebbistatin may impart on the myofilament of mouse cardiomyocytes.

Another limitation to this newly developed culture method is that the cultured cells may undergo alterations in fine structural and biochemical properties that cannot be detected by fluorescence microscope imaging and Western blotting. These alter-

ations may cause the cells to no longer contract in response to pacing after extended culture time and exposure to blebbistatin. Although the Nikolaev group has recently published an article showing that there is no difference in adrenergic-induced cAMP production in paced and quiescent cells, further explorations using FRET methodology of paced cells should be done in freshly isolated cells that come from transgenically expressing FRET sensor mice (Sprenger et al., 2015).

In summary, we have defined a general media formula to accommodate expression of a set of FRET biosensors during extended culture in adult mouse cardiomyocytes, allowing analysis of dynamic signaling transduction in living adult myocytes. Blebbistatin supplemented at a low concentration of 6.25 µM is effective at maintaining adult mouse cardiomyocyte morphology in culture for up to 50 h for FRET assays. The addition of HEPES and BSA to the media further reduces autofluorescent spotting of blebbistatin and improves cell quality, which improves overall signal-to-noise ratio during FRET experiments. This robust culturing process will allow for detailed single-cell time-sensitive measurements of signaling events. This opens the door to allow the myriad of genetic and pathological mouse models to be adopted for FRET experimentation. In the future, in addition to the biosensors tested here, subcellularly targeted FRET biosensors can be assessed for fine-tuned spatiotemporal dynamics inside mouse cardiomyocytes, allowing scientists to disentangle complicated signaling networks important in health and disease of cardiomyocytes.

References

Ackers-Johnson, M., P.Y. Li, A.P. Holmes, S.-M. O'Brien, D. Pavlovic, and R.S. Foo. 2016. A simplified, Langendorff-free method for concomitant isolation of viable cardiac myocytes and nonmyocytes from the adult mouse heart: novelty and significance. *Circ. Res.* 119:909–920. https://doi.org/10.1161/CIRCRESAHA.116.309202

Allen, M.D., and J. Zhang. 2006. Subcellular dynamics of protein kinase A activity visualized by FRET-based reporters. *Biochem. Biophys. Res. Commun.* 348:716–721. https://doi.org/10.1016/j.bbrc.2006.07.136

Barbagallo, F., B. Xu, G.R. Reddy, T. West, Q. Wang, Q. Fu, M. Li, Q. Shi, K.S. Ginsburg, W. Ferrier, et al. 2016. Genetically Encoded Biosensors Reveal PKA Hyperphosphorylation on the Myofilaments in Rabbit Heart Failure. *Circ. Res.* 119:931–943. https://doi.org/10.1161/CIRCRESAHA.116.308964

Bazzazi, H., L. Sang, I.E. Dick, R. Joshi-Mukherjee, W. Yang, and D.T. Yue. 2015. Novel fluorescence resonance energy transfer-based reporter reveals differential calcineurin activation in neonatal and adult cardiomyocytes. *J. Physiol.* 593:3865–3884. https://doi.org/10.1113/JP270510

Bers, D.M. 2002. Cardiac Na/Ca exchange function in rabbit, mouse and man: what's the difference? *J. Mol. Cell. Cardiol.* 34:369–373. https://doi.org/10.1006/jmcc.2002.1530

Bers, D.M. 2008. Calcium cycling and signaling in cardiac myocytes. *Annu. Rev. Physiol.* 70:23–49. https://doi.org/10.1146/annurev.physiol.70.113006.100455

Bork, N.I., and V.O. Nikolaev. 2018. cGMP Signaling in the Cardiovascular System: The Role of Compartmentation and Its Live Cell Imaging. *Int. J. Mol. Sci.* 19:801. https://doi.org/10.3390/ijms19030801

Börner, S., F. Schwede, A. Schlipp, F. Berisha, D. Calebiro, M.J. Lohse, and V.O. Nikolaev. 2011. FRET measurements of intracellular cAMP concentrations and cAMP analog permeability in intact cells. *Nat. Protoc.* 6:427–438. https://doi.org/10.1038/nprot.2010.198

Devic, E., Y. Xiang, D. Gould, and B. Kobilka. 2001. β-Adrenergic receptor subtype-specific signaling in cardiac myocytes from β(1) and β(2) adrenoceptor knockout mice. *Mol. Pharmacol.* 60:577–583.

DiPilato, L.M., and J. Zhang. 2009. The role of membrane microdomains in shaping beta2-adrenergic receptor-mediated cAMP dynamics. *Mol. Biosyst.* 5:832–837. https://doi.org/10.1039/b823243a

Dou, Y., P. Arlock, and A. Arner. 2007. Blebbistatin specifically inhibits actin-myosin interaction in mouse cardiac muscle. *Am. J. Physiol. Cell Physiol.* 293:C1148–C1153. https://doi.org/10.1152/ajpcell.00551.2006

Erickson, J.R., R. Patel, A. Ferguson, J. Bossuyt, and D.M. Bers. 2011. Fluorescence resonance energy transfer-based sensor Camui provides new insight into mechanisms of calcium/calmodulin-dependent protein kinase II activation in intact cardiomyocytes. *Circ. Res.* 109:729–738. https://doi.org/10.1161/CIRCRESAHA.111.247148

Farman, G.P., K. Tachampa, R. Mateja, O. Cazorla, A. Lacampagne, and P.P. de Tombe. 2008. Blebbistatin: use as inhibitor of muscle contraction. *Pflugers Arch.* 455:995–1005. https://doi.org/10.1007/s00424-007-0375-3

Fields, L.A., A. Koschinski, and M. Zaccolo. 2016. Sustained exposure to catecholamines affects cAMP/PKA compartmentalised signalling in adult rat ventricular myocytes. *Cell. Signal.* 28:725–732. https://doi.org/10.1016/j.cellsig.2015.10.003

Francis, G.L. 2010. Albumin and mammalian cell culture: implications for biotechnology applications. *Cytotechnology.* 62:1–16. https://doi.org/10.1007/s10616-010-9263-3

Good, N.E., G.D. Winget, W. Winter, T.N. Connolly, S. Izawa, and R.M. Singh. 1966. Hydrogen ion buffers for biological research. *Biochemistry.* 5:467–477. https://doi.org/10.1021/bi00866a011

Götz, K.R., J.U. Sprenger, R.K. Perera, J.H. Steinbrecher, S.E. Lehnart, M. Kuhn, J. Gorelik, J.-L. Balligand, and V.O. Nikolaev. 2014. Transgenic mice for real-time visualization of cGMP in intact adult cardiomyocytes. *Circ. Res.* 114:1235–1245. https://doi.org/10.1161/CIRCRESAHA.114.302437

Hall, A.R., and D.J. Hausenloy. 2016. Mitochondrial respiratory inhibition by 2,3-butanedione monoxime (BDM): implications for culturing isolated mouse ventricular cardiomyocytes. *Physiol. Rep.* 4:e12606. https://doi.org/10.14814/phy2.12606

Jian, Z., H. Han, T. Zhang, J. Puglisi, L.T. Izu, J.A. Shaw, E. Onofiok, J.R. Erickson, Y.-J. Chen, B. Horvath, et al. 2014. Mechanochemotransduction during cardiomyocyte contraction is mediated by localized nitric oxide signaling. *Sci. Signal.* 7:ra27. https://doi.org/10.1126/scisignal.2005046

Jian, Z., Y.-J. Chen, R. Shimkunas, Y. Jian, M. Jaradeh, K. Chavez, N. Chiamvimonvat, J.C. Tardiff, L.T. Izu, R.S. Ross, and Y. Chen-Izu. 2016. In Vivo Cannulation Methods for Cardiomyocytes Isolation from Heart Disease Models. *PLoS One.* 11:e0160605. https://doi.org/10.1371/journal.pone.0160605

Kabaeva, Z., M. Zhao, and D.E. Michele. 2008. Blebbistatin extends culture life of adult mouse cardiac myocytes and allows efficient and stable transgene expression. *Am. J. Physiol. Heart Circ. Physiol.* 294:H1667–H1674. https://doi.org/10.1152/ajpheart.01144.2007

Képiró, M., B.H. Várkuti, L. Végner, G. Vörös, G. Hegyi, M. Varga, and A. Málnási-Csizmadia. 2014. Para-nitroblebbistatin, the non-cytotoxic and photostable myosin II inhibitor. *Angew. Chem. Int. Ed. Engl.* 53:8211–8215. https://doi.org/10.1002/anie.201403540

King, N.M.P., M. Methawasin, J. Nedrud, N. Harrell, C.S. Chung, M. Helmes, and H. Granzier. 2011. Mouse intact cardiac myocyte mechanics: crossbridge and titin-based stress in unactivated cells. *J. Gen. Physiol.* 137:81–91. https://doi.org/10.1085/jgp.201010499

Klarenbeek, J., J. Goedhart, A. van Batenburg, D. Groenewald, and K. Jalink. 2015. Fourth-generation epac-based FRET sensors for cAMP feature exceptional brightness, photostability and dynamic range: characterization of dedicated sensors for FLIM, for ratiometry and with high affinity. *PLoS One.* 10:e0122513. https://doi.org/10.1371/journal.pone.0122513

Kolega, J. 2004. Phototoxicity and photoinactivation of blebbistatin in UV and visible light. *Biochem. Biophys. Res. Commun.* 320:1020–1025. https://doi.org/10.1016/j.bbrc.2004.06.045

Kovács, M., J. Tóth, C. Hetényi, A. Málnási-Csizmadia, and J.R. Sellers. 2004. Mechanism of blebbistatin inhibition of myosin II. *J. Biol. Chem.* 279:35557–35563. https://doi.org/10.1074/jbc.M405319200

Lomas, O., M. Brescia, R. Carnicer, S. Monterisi, N.C. Surdo, and M. Zaccolo. 2015. Adenoviral transduction of FRET-based biosensors for cAMP in primary adult mouse cardiomyocytes. *Methods Mol. Biol.* 1294:103–115. https://doi.org/10.1007/978-1-4939-2537-7_8

Louch, W.E., K.A. Sheehan, and B.M. Wolska. 2011. Methods in cardiomyocyte isolation, culture, and gene transfer. *J. Mol. Cell. Cardiol.* 51:288–298. https://doi.org/10.1016/j.yjmcc.2011.06.012

Luo, J., Z.-L. Deng, X. Luo, N. Tang, W.-X. Song, J. Chen, K.A. Sharff, H.H. Luu, R.C. Haydon, K.W. Kinzler, et al. 2007. A protocol for rapid generation of recombinant adenoviruses using the AdEasy system. *Nat. Protoc.* 2:1236–1247. https://doi.org/10.1038/nprot.2007.135

Madhvani, R.V., Y. Xie, A. Pantazis, A. Garfinkel, Z. Qu, J.N. Weiss, and R. Olcese. 2011. Shaping a new Ca²⁺ conductance to suppress early afterdepolarizations in cardiac myocytes. *J. Physiol.* 589:6081–6092. https://doi.org/10.1113/jphysiol.2011.219600

Mikulich, A., S. Kavaliauskiene, and P. Juzenas. 2012. Blebbistatin, a myosin inhibitor, is phototoxic to human cancer cells under exposure to blue light. *Biochim. Biophys. Acta.* 1820:870–877. https://doi.org/10.1016/j.bbagen.2012.04.003

Ni, Q., D.V. Titov, and J. Zhang. 2006. Analyzing protein kinase dynamics in living cells with FRET reporters. *Methods.* 40:279–286. https://doi.org/10.1016/j.ymeth.2006.06.013

Nikolaev, V.O., S. Gambaryan, and M.J. Lohse. 2006. Fluorescent sensors for rapid monitoring of intracellular cGMP. *Nat. Methods.* 3:23–25. https://doi.org/10.1038/nmeth816

Nikolaev, V.O., A. Moshkov, A.R. Lyon, M. Miragoli, P. Novak, H. Paur, M.J. Lohse, Y.E. Korchev, S.E. Harding, and J. Gorelik. 2010. β2-Adrenergic receptor redistribution in heart failure changes cAMP compartmentation. *Science.* 327:1653–1657. https://doi.org/10.1126/science.1185988

Ostap, E.M. 2002. 2,3-Butanedione monoxime (BDM) as a myosin inhibitor. *J. Muscle Res. Cell Motil.* 23:305–308. https://doi.org/10.1023/A:1022047102064

Riehle, C., and E.D. Abel. 2016. Insulin Signaling and Heart Failure. *Circ. Res.* 118:1151–1169. https://doi.org/10.1161/CIRCRESAHA.116.306206

Russwurm, M., F. Mullershausen, A. Friebe, R. Jäger, C. Russwurm, and D. Koesling. 2007. Design of fluorescence resonance energy transfer (FRET)-based cGMP indicators: a systematic approach. *Biochem. J.* 407:69–77. https://doi.org/10.1042/BJ20070348

Sadayappan, S., H. Osinska, R. Klevitsky, J.N. Lorenz, M. Sargent, J.D. Molkentin, C.E. Seidman, J.G. Seidman, and J. Robbins. 2006. Cardiac myosin binding protein C phosphorylation is cardioprotective. *Proc. Natl. Acad. Sci. USA.* 103:16918–16923. https://doi.org/10.1073/pnas.0607069103

Sakamoto, T., J. Limouze, C.A. Combs, A.F. Straight, and J.R. Sellers. 2005. Blebbistatin, a myosin II inhibitor, is photoinactivated by blue light. *Biochemistry.* 44:584–588. https://doi.org/10.1021/bi0483357

Schaffer, S.W., C.J. Jong, K.C. Ramila, and J. Azuma. 2010. Physiological roles of taurine in heart and muscle. *J. Biomed. Sci.* 17(Suppl 1):S2. https://doi.org/10.1186/1423-0127-17-S1-S2

Sich, N.M., T.J. O'Donnell, S.A. Coulter, O.A. John, M.S. Carter, C.R. Cremo, and J.E. Baker. 2010. Effects of actin-myosin kinetics on the calcium sensitiv-

ity of regulated thin filaments. *J. Biol. Chem.* 285:39150–39159. https://doi.org/10.1074/jbc.M110.142232

Sledź, P., R. Kamiński, M. Chruszcz, M.D. Zimmerman, W. Minor, and K. Woźniak. 2010. An experimental charge density of HEPES. *Acta Crystallogr. B.* 66:482–492. https://doi.org/10.1107/S0108768110023025

Soto, D., V. De Arcangelis, J. Zhang, and Y. Xiang. 2009. Dynamic protein kinase A activities induced by β-adrenoceptors dictate signaling propagation for substrate phosphorylation and myocyte contraction. *Circ. Res.* 104:770–779. https://doi.org/10.1161/CIRCRESAHA.108.187880

Sprenger, J.U., R.K. Perera, J.H. Steinbrecher, S.E. Lehnart, L.S. Maier, G. Hasenfuss, and V.O. Nikolaev. 2015. In vivo model with targeted cAMP biosensor reveals changes in receptor-microdomain communication in cardiac disease. *Nat. Commun.* 6:6965. https://doi.org/10.1038/ncomms7965

Surdo, N.C., M. Berrera, A. Koschinski, M. Brescia, M.R. Machado, C. Carr, P. Wright, J. Gorelik, S. Morotti, E. Grandi, et al. 2017. FRET biosensor uncovers cAMP nano-domains at β-adrenergic targets that dictate precise tuning of cardiac contractility. *Nat. Commun.* 8:15031. https://doi.org/10.1038/ncomms15031

Swift, L.M., H. Asfour, N.G. Posnack, A. Arutunyan, M.W. Kay, and N. Sarvazyan. 2012. Properties of blebbistatin for cardiac optical mapping and other imaging applications. *Pflugers Arch.* 464:503–512. https://doi.org/10.1007/s00424-012-1147-2

Takao, K., K. Okamoto, T. Nakagawa, R.L. Neve, T. Nagai, A. Miyawaki, T. Hashikawa, S. Kobayashi, and Y. Hayashi. 2005. Visualization of synaptic Ca2+/calmodulin-dependent protein kinase II activity in living neurons. *J. Neurosci.* 25:3107–3112. https://doi.org/10.1523/JNEUROSCI.0085-05.2005

Várkuti, B.H., M. Képiró, I.Á. Horváth, L. Végner, S. Ráti, Á. Zsigmond, G. Hegyi, Z. Lenkei, M. Varga, and A. Málnási-Csizmadia. 2016. A highly soluble, non-phototoxic, non-fluorescent blebbistatin derivative. *Sci. Rep.* 6:26141. https://doi.org/10.1038/srep26141

Wang, Q., Y. Liu, Q. Fu, B. Xu, Y. Zhang, S. Kim, R. Tan, F. Barbagallo, T. West, E. Anderson, et al. 2017. Inhibiting Insulin-Mediated β2-Adrenergic Receptor Activation Prevents Diabetes-Associated Cardiac Dysfunction. *Circulation.* 135:73–88. https://doi.org/10.1161/CIRCULATIONAHA.116.022281

Wright, P.T., V.O. Nikolaev, T. O'Hara, I. Diakonov, A. Bhargava, S. Tokar, S. Schobesberger, A.I. Shevchuk, M.B. Sikkel, R. Wilkinson, et al. 2014. Caveolin-3 regulates compartmentation of cardiomyocyte beta2-adrenergic receptor-mediated cAMP signaling. *J. Mol. Cell. Cardiol.* 67:38–48. https://doi.org/10.1016/j.yjmcc.2013.12.003

Zhou, Y.-Y., S.-Q. Wang, W.-Z. Zhu, A. Chruscinski, B.K. Kobilka, B. Ziman, S. Wang, E.G. Lakatta, H. Cheng, and R.-P. Xiao. 2000. Culture and adenoviral infection of adult mouse cardiac myocytes: methods for cellular genetic physiology. *Am. J. Physiol. Heart Circ. Physiol.* 279:H429–H436. https://doi.org/10.1152/ajpheart.2000.279.1.H429

Zimmermann, K.C., C. Bonzon, and D.R. Green. 2001. The machinery of programmed cell death. *Pharmacol. Ther.* 92:57–70. https://doi.org/10.1016/S0163-7258(01)00159-0